RESEARCH ARTICLE

Experimental Validation of Feedback PI Controllers for Multi-Rotor Wind Energy Conversion Systems

MOURAD YESSEF[1], **HABIB BENBOUHENNI**[2], **MOHAMMED TAOUSSI**[3], **AHMED LAGRIOUI**[4], **ILHAMI COLAK**[2], **BADRE BOSSOUFI**[1], **AND THAMER A. H. ALGHAMDI**[5,6]

[1]LIMAS Laboratory, Faculty of Sciences Dhar El Mahraz, Sidi Mohamed Ben Abdellah University, Fes 30000, Morocco
[2]Department of Electrical and Electronics Engineering, Faculty of Engineering and Architecture, Nişantaşı University, 34481 İstanbul, Turkey
[3]Higher School of Technology, Sidi Mohamed Ben Abdellah University, Fes 30000, Morocco
[4]Higher National School of Arts and Trades (ENSAM), University of Moulay Ismail, Meknes 50000, Morocco
[5]Wolfson Centre for Magnetics, School of Engineering, Cardiff University, CF24 3AA Cardiff, U.K.
[6]Electrical Engineering Department, School of Engineering, Albaha University, Al Baha 65779, Saudi Arabia

Corresponding authors: Mourad Yessef (mourad.yessef@usmba.ac.ma) and Thamer A. H. Alghamdi (alghamdit1@cardiff.ac.uk)

ABSTRACT This new paper describes an experimental investigation of a proportional-integral (PI) controller that uses feedback control to regulate an energy system that uses multi-rotor wind energy systems. Pulse width modulation (PWM) is used by the proposed controller to control the power of the doubly-fed induction generator controlled by direct power control (DPC), which is intended to regulate and control the inverter. The proposed strategy differs from the traditional DPC strategy. The proposed control was studied in the case of variable wind speed, where the MATLAB and Dspace 1104 environment was used to implement this proposed feedback PI (FPI) controller, with a comparison with the proposed control technique and some existing works. The suggested FPI controller outperforms the traditional controller and certain other controllers in terms of lowering energy ripples, overshoot, steady-state error (SSE), response time, and the total harmonic distortion (THD) of supplied system currents, as demonstrated by experimental and simulation results. The THD value of current was reduced by 64.86% and 69.44% in the two proposed tests compared to the traditional DPC technique. Also, the value of ripples and overshoot of active power was reduced compared to the DPC method by 95.42% and 90.86%, respectively, in the case of step wind speeds. Moreover, ripples and SSE of reactive powers compared to the DPC technique were reduced by 37.51% and 84.13%, respectively. These high ratios indicate the high performance of the proposed DPC-FPI technique in enhancing the features of the system in contrast to the conventional DPC technique.

INDEX TERMS Multi-rotor wind energy system, feedback control, direct power control, doubly-fed induction generator, proportional-integral controller.

NOMENCLATURE

DPC	Direct power control.
WS	Wind speed.
PWM	Pulse width modulation.
MRWT	Multi-rotor wind turbine.
WE	Wind energy.
MPPT	Maximum power point tracking.
SMC	Sliding mode control.
FPI	Feedback proportional-integral controller.
DTC	Direct torque control.
SC	Synergetic control.
FL	Fuzzy logic.
BC	Backstepping control.
NNs	Neural networks.
THD	Total harmonic distortion.
DFIG	Doubly-fed induction generator.
HC	Hysteresis comparator.
LT	Lookup table.
GA	Genetic algorithm.
STC	Super-twisting control.

The associate editor coordinating the review of this manuscript and approving it for publication was Jiann-Jong Chen.

I. INTRODUCTION

One of the key elements contributing to the rebirth of nations and governments is energy, as the issue of electrical energy is considered one of the most prominent themes and topics in the current era due to its sensitivity and great importance in the industrial and economic field. Electrical energy is the energy that has changed the world for the better and provided a better life for humanity, as several sources can be used to obtain it. These sources can be divided and separated into two branches: renewable sources and non-renewable sources. The use of non-renewable power resources such as gas to generate electrical energy causes several problems such as global warming. In addition to the high costs of producing and consuming electrical energy, which is undesirable, which has made governments look for other solutions. One of the most popular solutions put forth in recent years to replace conventional sources and combat the rising demand for electrical energy consumption is the use of renewable energy and power resources, specifically wind and solar energy. In addition to the possibility of reducing the costs of producing and consuming electrical energy. As is known, wind energy (WE) is clean, inexpensive, and easy to use, as turbines are utilized to convert WE into mechanical energy. The latter is utilized or converted by electric generators into electrical energy, where the amount of energy produced is largely related and linked to wind speed (WS).

The most widely used generator can be mentioned as the doubly-fed induction generator (DFIG) [1], as it is characterized by several advantages that make it superior to all other generators. Comparing this generator to many others, its advantages are its low cost, great durability, and simplicity of control [2]. This generator has a feature that differs from other generators, which is that it controls the resulting energy by feeding the moving part of the machine, as two different inverters are used for this purpose. This generator is also connected directly to the network without the need to use transformers or inverters, which makes costs lower compared to using a synchronous generator. Therefore, focus was placed in this work on its use in generating electrical energy using a multi-rotor wind turbine (MRWT) power and energy system [3]. MRWT is a new turbine technology that has recently emerged as an alternative solution to traditional turbines for producing electrical energy from wind, as it is characterized by distinctive and effective performance compared to traditional turbines. This new technology has been discussed in detail in several different works [4], [5], [6], [7], where all of these works confirm the superiority of these turbines over traditional turbines.

According to the work done in [8], the MRWT turbine has sufficient capacity to gain more energy from the wind than traditional turbines, which makes it the appropriate solution in the future for generating energy from wind. In addition, the use of this type leads to reducing the area of wind farms and thus the costs, which is a good thing and makes this turbine the appropriate solution in this study to implement the proposed system. The MRWT turbine has the ability to overcome unwanted winds in wind farms that arise between the turbines, as these turbines are not affected by these winds, which makes their yield large and unchangeable. Also, the use of MRWT makes the power system more stable compared to conventional turbines. The negative of these turbines is the high costs due to the presence of two or more turbines together, as there are a large number of mechanical components, which makes regular maintenance expensive [9].

Traditionally, the strategy of direct control of distinct quantities is a strategy characterized by simplicity and rapid dynamic response, which makes it one of the most famous approach in the field of system control, as there are two types of this strategy: DTC (Direct torque Control) and DPC (Direct power control) [10]. These strategies have fewer gains, making them easy to adjust and inexpensive, which is a good thing. The DPC and DTC strategies are among the most prominent linear control strategies used in the field of controlling electrical machines, especially in the field of renewable energies. These strategies depend on the use of a lookup table (LT) to regulate and control the operation of the inverter machine, and traditional controllers of the type hysteresis comparators (HCs) are used to control the characteristic quantities (Energy and Torque) [11]. Therefore, there are no complex calculations in these strategies that hinder their application to the systems. The DPC strategy has the same principle, idea, and structure as the DTC strategy, the difference between which lies in the amounts controlled. In the DPC strategy, power is controlled, and in the DTC strategy, torque and flow are controlled. So, the focus will be on DPC technique in this work to control the energy generated by the MRWT-based WE system. According to the work done in [11], the DPC strategy has many disadvantages that can be identified in the following points: 1) the presence of large fluctuations at the power level, 2) low current quality, 3) the use of power estimation, which makes it tied to the system parameters, 4) low durability, 5) The current has a high value of total harmonic distortion (THD), 6) The presence of variable and high frequencies at the current level.

In order to overcome these defects, several intelligent strategies were used for this purpose, as genetic algorithms (GAs) [12], neural networks (NNs) [13], particle swarm optimization (PSO) [14], and fuzzy logic (FL) [15] were used. These artificial intelligence techniques, which mainly rely on experience, were employed to lessen the energy ripples' intensity and the THD value of current. Because the DPC strategy's parameters were determined using these strategies—like GA and PSO—the resulting strategies are desirable because they are straightforward and simple to implement. Both FL and NNs were used to generate the pulses needed to operate the inverter and thus compensate for the use of LT. By employing these techniques, power ripples are greatly decreased and the DPC strategy's robustness is

increased. The negative of these strategies is that there is no rule that determines how to use them to obtain good results, as there is no mathematical rule that determines the number of FL rules or the number of internal layers and neurons needed, and this is undesired. Furthermore, these suggested intelligent strategies depend on capacity estimation, which means that in the event of a system malfunction—which is undesirable—the DPC strategy will be impacted. Therefore, it is necessary to search for other strategies that are more efficient and performant in overcoming the problems of the DPC method.

There are those who proposed a solution in nonlinear strategies such as synergetic command (SC) [16], back-stepping command (BC) [17], super-twisting command (STC) [18], sliding mode command (SMC) [19], and third-order SMC [20] to increase the performance of the DPC strategy, where both LT and HCs were dispensed with. In these proposed nonlinear strategies, space vector modulation (SVM) or pulse width modulation (PWM) is utilized and employed to regulate and control the inverter of the DFIG. Using these strategies mentioned above increased the degree of complexity of the traditional DPC strategy and the difficulty of real embedded implementation, such as using SMC and BC techniques, where it is noted that there are a significant number of gains, which makes adjusting the dynamic response somewhat complicated. Also, using these strategies makes the DPC strategy tied to the DFIG parameters, which is undesirable and makes the strategy give unsatisfactory results in the event of a malfunction in the energy conversion system. However, the use of these strategies led to a significant reduction in energy ripples and a reduction in the THD value of current compared to the traditional DPC strategy. In the durability tests, it is noted that there is a significant increase on the ripple value and the THD value, which is undesirable, causes disturbances in operation and significantly reduces the life of the system.

Some works have suggested combining strategies to obtain distinctive performance for the DPC strategy, where three or two strategies that are different or similar in principle are combined. In the work [21], the author used a combination of SC method and SMC approach to overcome and remedy the problems of DPC technique of DFIG-MRWT, where he used the resulting strategy (SC-SMC) to regulate the DFIG powers. The approach is straightforward and preserves the traditional strategy's ease of completion. This strategy relies on estimating powers, which makes it give unsatisfactory results in a durability test, where an increase in torque/power ripples and a decrease in the quality of the current are observed. The DPC-SC-SMC strategy was applied to a 1.5 MW DFIG-MRWT with variable WS for the purpose of studying efficiency, durability, and performance compared to the DPC strategy. The obtained simulation results highlight the distinctive performance of the DPC-SC-SMC strategy in improving system characteristics compared to the traditional DPC strategy. Nonetheless, the issue of ripples persists,

particularly in the case of a system malfunction. Another integration was done in [22] to control the capabilities and overcome the drawbacks of the traditional DPC strategy, as the author used both SMC and BC techniques for this purpose. The structure and guiding principles of the DPC-BC-SMC strategy differ from those of the traditional DPC strategy. This strategy uses the PWM technique to control the RSC of DFIG and uses a BC-SMC technique to regulate the DFIG power. Complexity, implementation difficulty, and a high number of gains are characteristics of the suggested strategy that make it challenging to control the dynamic response. This strategy uses the same estimation equations found in the DPC strategy. The MATLAB/simulink environment was employed to implement the proposed strategy, and a variable WS was used to complete the study. The outcomes of the simulation showed that the suggested strategy outperformed the conventional DPC strategy in terms of enhancing current quality. However, the undesired issue of energy ripples persists.

In [23] and [24], the PWM technique was employed to generate the control pulses required to operate the RSC of DFIG. Both the fractional-order NNs and fractional-order FL techniques were utilized as new controls to replace the traditional controls. The proposed strategies are characterized by simplicity and high robustness due to the use of the combination between fractional-order control and intelligent techniques. In these strategies, the maximum power point tracking (MPPT) technique based on PI controller was used in order to obtain the reference value for active power. The calculated reference value is used to calculate the error in active power, as the error value in active power is considered an input to the proposed controls. These proposed strategies were implemented in the MATLAB environment, with a comparative study between the DPC strategy and some existing controls in terms of the percentage of response time reduction, ripples, steady-state error (SSE) and overshoot of DFIG power. The results obtained demonstrate the high performance of the proposed controls in improving the system characteristics compared to several works. The negative of these strategies lies in estimating capabilities, as they use the same estimation equations, which makes them provide unsatisfactory results in the event of a malfunction in the system. In addition to the smart strategies in themselves, these strategies depend on experience and there are no rules to help in their application, which makes the matter somewhat complicated and difficult to determine the necessary number of FL technique rules or the number of neurons needed. In [25], GA technique, terminal sliding surface technique, and PI controller were used to overcome the problems of the traditional DPC strategy of DFIG-MRWT systems. The obtained strategy is characterized by high robustness and ease of implementation, as the MATLAB environment was used for the purpose of implementation, with the use of several tests to verify its behavior. The results obtained showed the high performance of the proposed strategy, as it provided high reduction rates compared to the traditional

strategy and some actions. PI controller and SC technique were combined to control DFIG power and overcome the drawbacks of the traditional DPC strategy [26], where GA technique was utilized to determine the gain values of the proposed controller. The DPC-PI-SC-GA strategy is distinguished by high durability and great efficiency in reducing power ripples and improving current quality compared to the traditional DPC strategy. To control the guest energy system, there were several challenges facing the control of these systems. The most prominent of these challenges are ease of control, ease of implementation, number of acquisitions, durability, distinctive performance, and cost.

All this factor makes the control technique of the system of great importance, as controlling the organs contributes to reducing the cost of the system and reducing the cost of production and energy consumption. Among the simplest solutions that have been proposed to overcome the shortcomings of the traditional DPC strategy are the PI(1+PI) [27] and proportional-derivative-(1+PI) technique [28] techniques, as the two proposed ideas are very simple and of great importance in the field of control. These two proposed DPC strategies were utilized to remedy and overcome the shortcomings and disadvantages of the DFIG-MRWT system, as they provided very satisfactory reduction rates compared to the traditional DPC strategy and some existing works.

The use of power estimation causes ripples and fluctuations at the level of active and reactive power, which is a drawback to these strategies despite their simplicity, affordability, and ease of embedded real time implementation. In addition to having a significant number of gains, which is not desirable. Therefore, it is necessary to search for another solution that is distinguished by simplicity, outstanding performance, durability, efficiency in reducing the intensity of energy waves, fewer gains, ease of real time embedded implementation, and low cost. All these features are necessary to choose the appropriate control to overcome and remedy the disadvantages of the DPC strategy. So, the completed work deals with a new DPC strategy based on the use of a new linear controller to improve and ameliorate the performance and efficiency of the DPC technique of DFIG-MRWT. The new linear controller is a PI controller based on feedback technique, as this controller is considered a new strategy that has not been discussed before in the field of control, particularly in the field of renewable powers resources. So the main contribution of the paper is to propose the feedback PI (FPI) controller as a suitable solution to overcome and remedy the drawbacks and problems of the traditional DPC strategy of DFIG-MRWT. This proposed controller has several advantages, including simplicity, durability, ease of embedded real time implementation, few gains, and distinctive performance with a fast dynamic response, which makes it a suitable solution in this work. In addition, there are other contributions made in this paper that can be identified in the following points: 1) Experimentally

implementing the proposed controller using Dspace 1104, 2) Comparing the proposed DPC strategy with the traditional DPC strategy and some existing works, 3) Improving the quality of power/current, 4) Reducing the THD of current, and 5) Minimizing the value of overshoot and SSE of DFIG energy.

The research contained seven sections, the second section talked about the obstetrics system proposed for the study. In the third section, the proposed DPC control principle and its characteristics are presented. The DPC-FPI strategy is detailed and its mathematical model is presented in Section IV. The fifth section deals with numerical simulation of the proposed DPC-FPI strategy with a comparative study with the traditional DPC strategy. Experimental results are listed in Section VI. The paper ends with a conclusions section, where all findings related to the work performed are collected.

II. PROPOSED WE SYSTEM

The WE system proposed in this paper depends on the use of an MRWT turbine to gain energy from the wind and provide the generator with sufficient energy to produce electrical energy, where a generator with a capacity of 1.5 megawatts is used. DFIG and MRWT are considered the main sections of this system, and the mathematical model will be given to them to complete the necessary simulation.

A. TURBINE MODEL

MRWT is a modern turbine that has the ability to provide greater WE as a result of using several turbines. The use of these turbines contributes to significantly reducing the area of wind farms and thus reducing the costs of constructing wind farms [3], [8], which leads to reducing the costs of producing and consuming electrical energy. In addition, these turbines are more stable than traditional turbines, as they are not affected by the wind generated between the turbines in wind farms, making them one of the most reliable solutions in the future for producing electrical energy. Compared to traditional turbines, MRWTs are difficult to control, expensive, require constant periodic maintenance, and contain a large number of mechanical parts. To control this turbine, the MPPT strategy is used for this purpose, as this strategy was detailed in the work [29]. As is known, the MPPT strategy is used for the purpose of controlling MRWT and obtaining more energy from wind. Also, protect the MRWT from strong winds. MRWT is considered to have great durability against strong winds compared to traditional turbines, which makes it one of the most prominent solutions that can be relied upon in the field of electric power generation in the future, as these turbines are considered a new technology and in continuous development. According to the work [27], [28], the torque of this turbine can be expressed by Equation (1). So the torque is a sum of the torques of the turbines forming the mother turbine.

$$T_t = T_1 + T_2 \tag{1}$$

Equation (2) shows the torque of the two turbines, where the torque value depends on the dimensions of each turbine.

$$\begin{cases} T_2 = \dfrac{C_p}{2\lambda_2^3} \, \rho \cdot \pi \cdot R_2^5 \cdot w_2^2 \\ T_1 = \dfrac{C_p}{2\lambda_1^3} \, \rho \cdot \pi \cdot R_1^5 \cdot w_1^2 \end{cases} \tag{2}$$

The total capacity of the turbine is represented in Equation (3).

$$P_t = P_1 + P_2 \tag{3}$$

The power generated by each turbine can be calculated using Equation (4) [12], [21].

$$\begin{cases} P_{St} = \dfrac{C_p(\beta, \lambda)}{2} \, \rho \cdot S_{St} \cdot w_{St}^3 \\ P_{Lt} = \dfrac{C_p(\beta, \lambda)}{2} \, \rho \cdot S_{Lt} \cdot w_{Lt}^3 \end{cases} \tag{4}$$

Torque or power is related to a factor called coefficient of power (C_p), and this work is of great importance in determining the value of the energy gained from the wind. Equation (5) represents this coefficient for MRWT.

$$C_p(\beta, \lambda) = \frac{1}{0.08\beta + \lambda} + \frac{0.035}{\beta^3 + 1} \tag{5}$$

The parameter C_p is affected by two main factors: pitch angle (β) and tip speed ratio (λ), where it has the largest value when $\beta = 0°$. On the other hand, the value of this parameter increases as the tip speed ratio decreases. For each turbine, it can be expressed according to the Equation (6).

$$\begin{cases} \lambda_{St} = \dfrac{w_{St} \cdot R_{St}}{V_{ST}} \\ \lambda_{Lt} = \dfrac{w_{Lt} \cdot R_{Lt}}{V_{Lt}} \end{cases} \tag{6}$$

In MRWT, the WS of the two turbines forming the parent turbine is different, as each turbine has its own WS. The first turbine has a normal WS, while the second turbine has a WS given by the Equation (7). This speed is related to the distance (x) between the two turbines, as the distance between the two turbines in this paper is estimated at 15 meters because the turbine is under major study and its capacity is estimated at 1.5 megawatts. Moreover, the WS of the second turbine is related to the WS ($V1$) before the first turbine and a constant factor (C_T) of 0.9 [8], [27].

$$V_2 = V_1 \left(1 - \frac{1 - \sqrt{(1 - C_T)}}{2} \left(1 + \frac{2x}{\sqrt{1 + 4x^2}} \right) \right) \tag{7}$$

B. DFIG MODEL

The DFIG was relied upon because of the characteristics that distinguish it mentioned in [1] and [2], where the rotational speed can be controlled by feeding the moving part, which is a feature not found in other machines. The mathematical model of this generator is based on giving the relationships between flux, voltage, and current. In addition to the relationship between speed and torque. The Equations (8) to (10) represent these relationships that connect different quantities

$$\begin{cases} V_{dr} = R_r I_{dr} - w_r \Psi_{qr} + \dfrac{d}{dt} \Psi_{dr} \\ V_{qr} = R_r I_{qr} + w_r \Psi_{dr} + \dfrac{d}{dt} \Psi_{qr} \\ V_{qs} = R_s I_{qs} + w_s \Psi_{ds} + \dfrac{d}{dt} \Psi_{qs} \\ V_{ds} = R_s I_{ds} - w_s \Psi_{qs} + \dfrac{d}{dt} \Psi_{sd} \\ \Psi_{dr} = L_r I_{dr} + M I_{ds} \\ \Psi_{qr} = M I_{qs} + L_r I_{qr} \\ \Psi_{qs} = M I_{qr} + L_s I_{qs} \\ \Psi_{ds} = L_s I_{ds} + M I_{dr} \end{cases} \tag{8}$$

$$\begin{cases} T_e = J \times \dfrac{d\Omega}{dt} + f \times \Omega + T_r \\ T_r = 1.5p \times \dfrac{M}{L_s}(-\Psi_{sd} \times I_{rq} + \Psi_{sq} \times I_{rd}) \end{cases} \tag{9}$$

Power is related to voltage and current, and is estimated by measuring both voltage and current. Therefore, the Equation (10) is used to find the necessary power values for the control strategy.

$$\begin{cases} P_s = 1.5 \times (V_{qs} \times I_{qs} + I_{ds} \times V_{ds}) \\ Q_s = 1.5 \times (-I_{qs} \times V_{ds} + V_{qs} \times I_{ds}) \end{cases} \tag{10}$$

To enhance the generator's qualities, a number of alternative controllers have been suggested for it. These controllers vary in terms of complexity, ease of use, cost, durability, performance, and efficiency. One of the most prominent challenges facing the implementation of any control system is the presence of these features mentioned in the proposed FPI controller, as these features are of great importance in determining the cost of the system and the quality of the resulting energy. Therefore, it is necessary to focus on these characteristics to suggest the controller needed to be used to control capabilities.

III. SUGGESTED FPI CONTROLLER

Based on the application of a PI controller, a new linear controller is suggested in this section as a workable solution in this paper. The latter is the best option for a variety of systems because of its many benefits, including its simplicity, low number of gains, ease of implementation, affordability, and its quick dynamic speed. The PI controller's mathematical form is represented by Equation (11).

$$u(t) = K_p . e(t) + K_i . \int e(t) . dt \tag{11}$$

Equation (11) can be illustrated using Figure 1 to simplify understanding and to illustrate the changes that will occur to this controller to implement the new controller.

The proposed controller is a change in the PI controller, where feedback action represented in Equation (12) is used to increase the durability and performance of the PI controller.
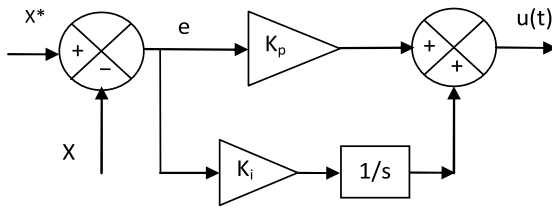
FIGURE 1. PI controller.

To simplify understanding the proposed method and clarify the shape of the new controller, Figure 2 is used for this purpose.

$$E = Y - X \tag{12}$$
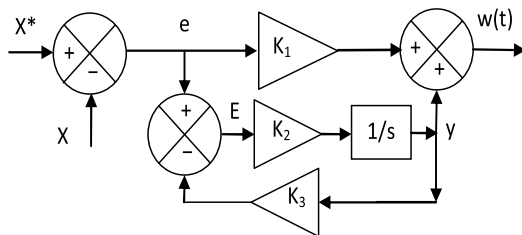
FIGURE 2. FPI controller.

By comparing Figures 1 and 2, the proposed FPI controller is different from the traditional controller in principle and mathematical form. In Table 1, the differences and similarities between the two controls are given.

TABLE 1. Comparison between controllers PI and FPI.

Properties	PI controller	FPI controller
Number of gains	2 (Ki and Kp)	3 (K1, K2, and K3)
number of integrals	1	1
Number of errors	1 (e)	2 (e and E)
Number of comparators	1	2
Number of feedback action	0	1

The suggested controller's mathematical model can be extracted from Figure 2, where the equation denotes the mathematical model that corresponds to this controller. The primary characteristics of this suggested FPI controller are its simplicity, ease of use, and affordability.

$$w(t) = K_1 . e(t) + K_2 . \int E(t) dt \tag{13}$$

where, e and E are the errors and K_1, K_2, and K_3 are the gains of FPI controller. Through these gains, the dynamic response can be controlled and changed, and smart strategies can be used to calculate it. Using smart strategies helps get better results. Equation (14) represents the mathematical model of the error (E), as it relates to the error e value.

$$E(t) = e(t) - K_3 . y \tag{14}$$
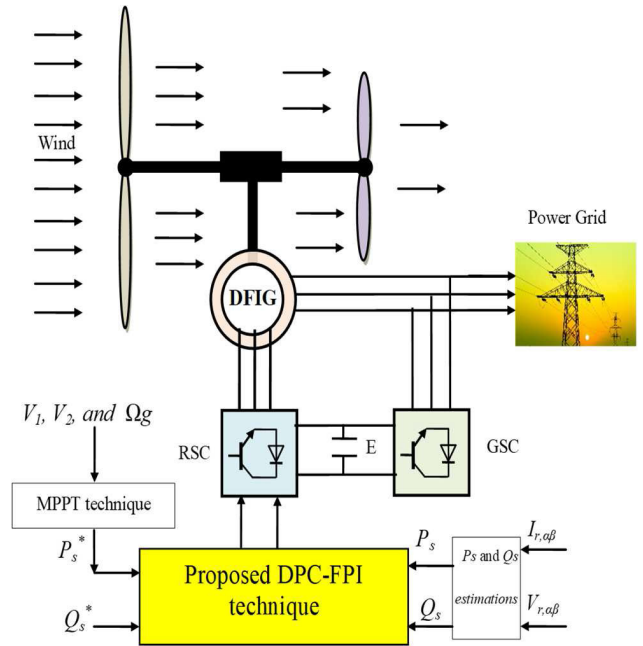
FIGURE 3. The designed DPC-FPI technique.

This proposed FPI controller will be designed and employed to improve and enhance the performance of the DPC technique of DFIG-MRWT system in the next part, where the necessary details for this proposed DPC-FPI strategy will be mentioned.

IV. PROPOSED DPC-FPI TECHNIQUE OF THE DFIG

The DPC-FPI strategy is among the most prominent contributions of this paper. It is considered a new work and has not been discussed previously, and it differs from the work done in [30] and some other work [12], [18], [27], [28]. This proposed strategy differs from traditional DPC technique in terms of idea, principle, and structure. The proposed FPI strategy does not use both the LT and two HCs, which makes it give distinctive performance compared to the DPC strategy. In this proposed DPC-FPI strategy, two FPI controllers are used to control DFIG energy. In addition to using the PWM technique to control the operation of the RSC of DFIG. Therefore, the proposed DPC-FPI strategy is distinguished by simplicity, low cost, small number of gains, quick dynamic response, and ease of embedded real time implementation. Figure 3 represents the proposed DPC-FPI strategy used in this paper to control the energy system.

The suggested DPC-FPI approach uses estimation of powers to compute the error, which is computed for both reactive and supplied active power. These errors are the inputs to the FPI controller of proposed DPC technique with PWM technique. The flux must first be estimated, and Equation (15) is used for this purpose. As is known, power is related to flux and current. Equation (16) represents the absolute value of the flux, as this value is calculated based on the components

in Equation (15).

$$
\begin{cases}
\Psi_{s\beta} = \int_0^t (V_s - R_s \times i_{s\beta})dt \\[2mm]
\Psi_{r\alpha} = \int_0^t (V_r - R_r \times i_{r\alpha})dt \\[2mm]
\Psi_{s\beta} = \int_0^t (V_s - R_s \times i_{s\beta})dt \\[2mm]
\Psi_{s\alpha} = \int_0^t (V_s - R_s \times i_{s\alpha})dt
\end{cases}
\tag{15}
$$

$$
\begin{cases}
|\Psi_r| = \sqrt{\left(\Psi_{r\beta}^2 + \Psi_{r\alpha}^2\right)} \\[2mm]
|\Psi_s| = \sqrt{\left(\Psi_{s\beta}^2 + \Psi_{s\alpha}^2\right)}
\end{cases}
\tag{16}
$$

Flux is related to voltage, so as voltage changes, flux changes with it. Equation (17) represents the relationship between flux and voltage, and this equation can be used to extract the flux value.

$$
\begin{cases}
|\overline{V_r}| = |\bar{\Psi}_r| \overline{\times} w_r \\[2mm]
|\overline{V_s}| = |\overline{\Psi_s}| \times w_s
\end{cases}
\tag{17}
$$

Using Equation (15), it is possible to extract the value of the angle that is used to control and control the Park transformation, as these angle values are considered necessary to accomplish the proposed DPC-FPI strategy, and Equation (18) represents how to calculate these angles based on the flux components.

$$
\begin{cases}
\theta r = \text{artg}\, \dfrac{\Psi_{r\beta}}{\Psi_{r\alpha}} \\[3mm]
\theta s = \text{artg}\, \dfrac{\Psi_{s\beta}}{\Psi_{s\alpha}}
\end{cases}
\tag{18}
$$

So, to estimate the capabilities, Equation (20) can be used for this purpose. This equation is the same equation used in the DPC strategy.

$$
\begin{cases}
Q_s = -\dfrac{3}{2}\left(\dfrac{V_s}{\sigma \times L_s} \times \Psi_{\beta r} - \dfrac{V_s \times L_m}{\sigma \times L_r \times L_s}\right) \\[3mm]
P_s = -\dfrac{3}{2} V_s \times \Psi_{r\beta} \times \dfrac{L_m}{\sigma \times L_r \times L_s}
\end{cases}
\tag{19}
$$

The stator flux can be expressed in another way, where the Equation (20) is used for this purpose.

$$
\begin{cases}
\Psi_{s\beta} = \sigma I_{r\beta} L_r \\[2mm]
\Psi_{s\alpha} = \sigma I_{r\alpha} L_r + \Psi_s \dfrac{M}{L_s}
\end{cases}
\tag{20}
$$

The DPC-FPI strategy aims to calculate voltage reference values, and these reference values are used by the PWM strategy to generate the pulses necessary to operate the RSC of DFIG. Therefore, the error in the capabilities is first determined according to the Equation (21). The Equation (13) of the proposed controller is used to determine the voltage reference values. So the Equation (22) can be relied upon to determine these reference values. Figures 4 and 5 represents

the proposed controllers to control power and reduce energy ripples. In this proposed DPC-FPI strategy, the MPPT strategy is used to determine the reference value for the active power and thus obtain the greatest energy gained from the wind to generate the greatest current value.

$$
\begin{cases}
e_{P_s} = P_s^* - P_s \\[2mm]
e_{Q_s} = Q_s^* - Q_s
\end{cases}
\tag{21}
$$

$$
\begin{cases}
V_{dr}^* = K_1 . e_{Q_s}(t) + K_2 . \int E_{Q_s}(t)dt \\[2mm]
V_{qr}^* = K_1 . e_{P_s}(t) + K_2 . \int E_{P_s}(t)dt
\end{cases}
\tag{22}
$$
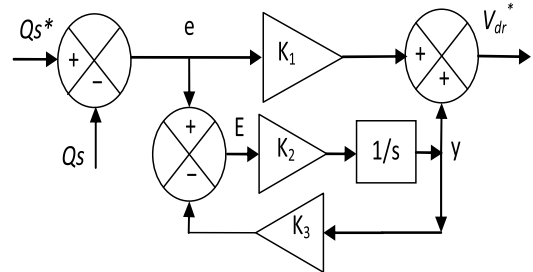
FIGURE 4. The designed FPI technique of Q_s.
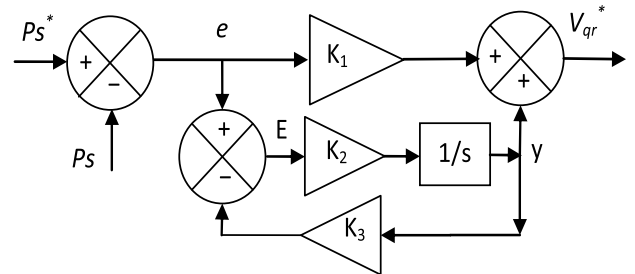
FIGURE 5. The designed FPI technique of P_s.

The proposed DPC-FPI strategy will be implemented experimentally using the MATLAB environment in the following sections to demonstrate its efficiency and ability to improve the quality of current and power.

V. NUMERICAL RESULTS

In this section, a numerical simulation of the proposed DPC-FPI strategy compared to the traditional DPC strategy is given, where the necessary numerical and graphical results to make the comparison are extracted. The DFIG parameters are as follows: $R_s = 0.012\ \Omega$, $P_{sn} = 1.5$ MW, $L_r = 0.0136$ H, $L_m = 0.0135$ H, $J = 1000\ \text{kg.m}^2$, 380/696 V, $R_r = 0.021\ \Omega$, 50 Hz, $L_s = 0.0137$ H, p=2, and $f_r = 0.0024$ Nm/s.

Variable WS with two different shapes is used to study the efficiency of the proposed DPC-FPI strategy in improving the quality of power and current.

A. STEPS WIND PROFILE

In this test, the characteristics of the proposed DPC-FPI strategy are studied according to the WS represented in

Figure 6, where the results obtained are represented in Figures 7 to 11. Through these shapes, the capabilities follow the references well (Figures 7 and 8) with the presence of ripples in the case of the DPC strategy compared to the DPC-FPI strategy. Reactive power does not change according to the change in WS. In addition, torque and current follow the change in the shape of active power perfectly, as the WS increases, the value of both torque and current increases (see Figures 9-11). It is noted that there are ripples in the determination, as these ripples are much smaller in the case of using the traditional DPC strategy. The currents take a sinusoidal shape, with an advantage over the proposed DPC-FPI strategy in terms of quality and undulations.
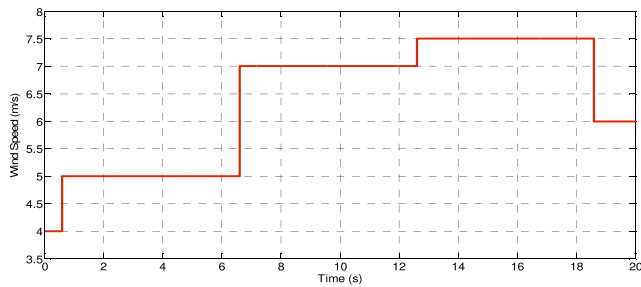
FIGURE 6. Steps WS profile.
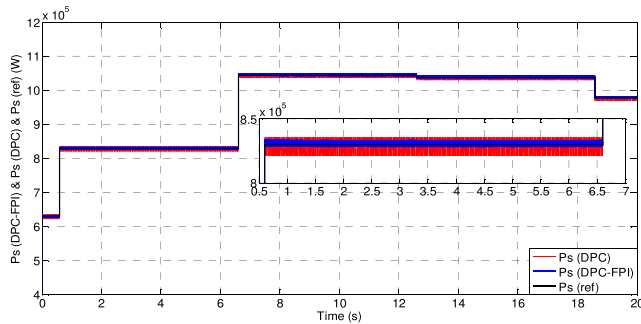
FIGURE 7. *Ps* of DPC-FPI and DPC.
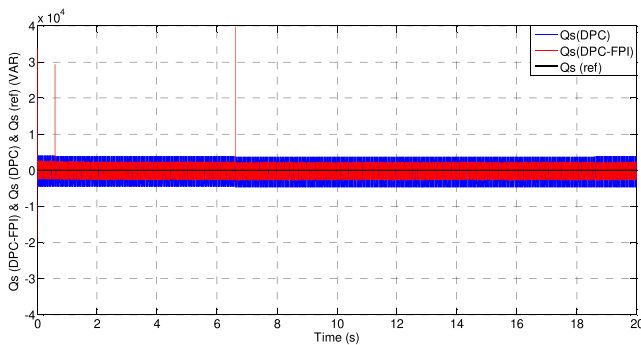
FIGURE 8. *Qs* of DPC-FPI and DPC.

In Figure 12, the value of THD of current is given for both strategies, where it is noted that the value of THD is 0.37and 0.13% for the traditional and proposed
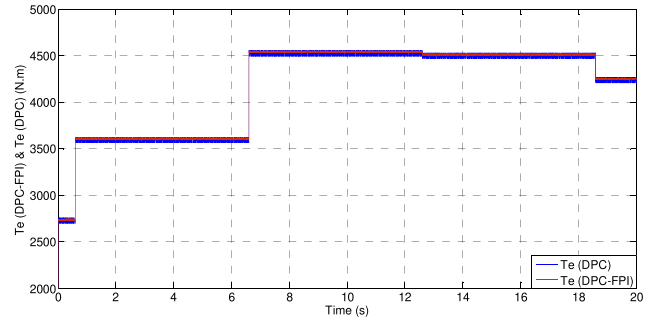
FIGURE 9. Torque.
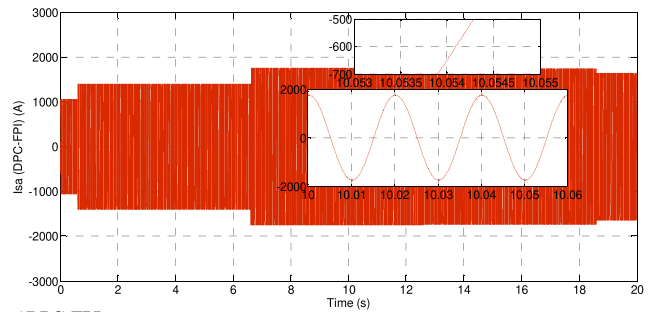
a)DPC-FPI
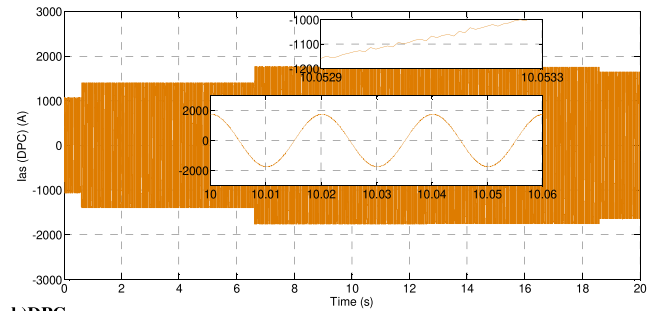
b)DPC

FIGURE 10. Current (Isa).

strategies, respectively. So, the proposed strategy reduced the value of THD compared to the traditional strategy, as the percentage of reduction in the value of THD was estimated at 64.86This high percentage indicates that the quality of the stream is better in the case of the proposed strategy. It also indicates the distinctive performance of the proposed strategy in improving the system characteristics compared to the traditional strategy. On the other hand, Figure 12 indicates that the value of the amplitude of the fundamental signal (50 Hz) of current is high if the proposed strategy is used compared to the traditional strategy, which is desirable. The value of this amplitude was 1389 A and 1394 A for both the traditional and the proposed strategy, respectively. So, the proposed strategy improved the value of the amplitude by an estimated rate of 0.35%, as this percentage is very small, but it expresses the superiority of the proposed strategy, which is a good thing.

Table 2 represents the numerical results of this test, where the values and percentages of ripple reduction, response time, overshoot, and SSE of *Ps* and *Qs* are given. From

a) DPC-FPI

b) DPC
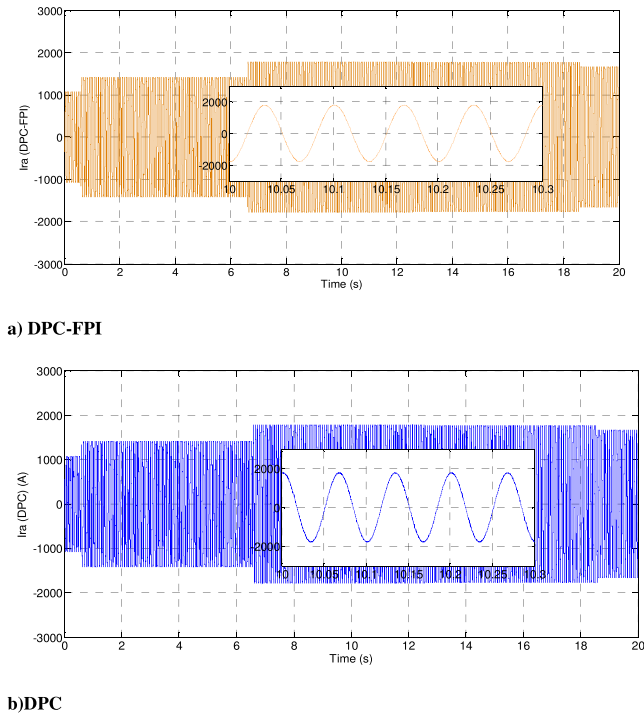
FIGURE 11. Current (*Ira*).

a) DPC-PI
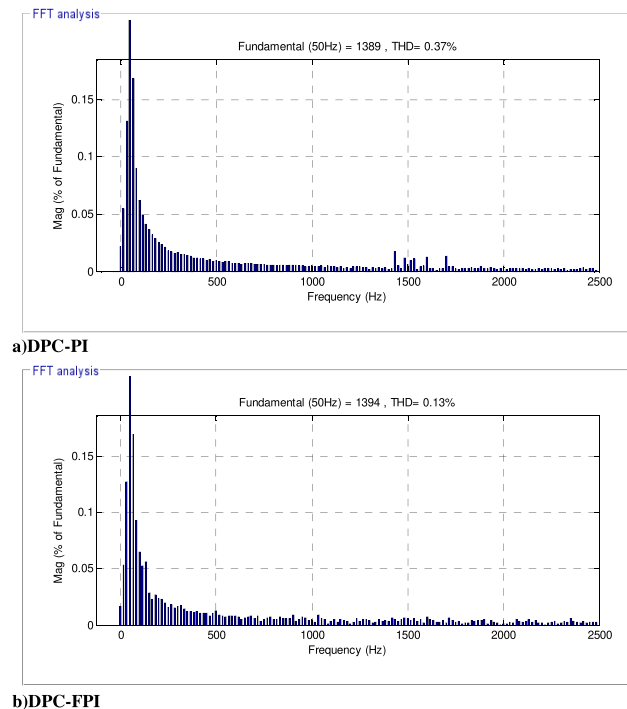
b) DPC-FPI

FIGURE 12. THD value of current (Test_1).

this table it is noted that the proposed DPC-FPI strategy provided satisfactory results for both ripples, SSE and overshoot of *Ps* and *Qs* and this is shown by the high reduction ratios. However, the proposed DPC-FPI strategy provided unsatisfactory results in terms of response time. The

traditional DPC strategy gave a good time compared to the DPC-FPI strategy.

TABLE 2. Value and ratios of power ripples, overshoot, SSE, and response time of both techniques in the first test.

		Ps (W)	*Qs* (VAR)
DPC	Ripples	5120	8050
	Overshoot	1015	230
	SSE	1130	2016
	Response time	0.85ms	0.96ms
DPC-FPI	Ripples	2120	5030
	Overshoot	630	860
	SSE	540	320
	Response time	1.70ms	1.85ms
Improvement Ratios	Ripples	58.60%	37.51%
	Overshoot	37.93%	-73.25%
	SSE	52.21%	84.13%
	Response time	-50%	-48.10%

B. VARIABLE WS PROFILE

In this test, a different WS is used than the first test to study the performance of the proposed DPC-FPI strategy, as the WS profile represented in Figure 13 is used for the purpose of completing this test. Figures 14-18 represent the graphical results of this test, as it is noted that the potential continues to follow the references well, with large ripples in the case of the traditional DPC strategy (Figures 14 and 15). but reactive power takes a fixed value and does not change with changes in WS, unlike active power, which changes according to changes in wind speed. Figure 16 represents the torque of the generator and it changes according to the change in WS. it increases with increasing WS and its value decreases with decreasing WS. it is also noted that there are large ripples at the level of torque in the traditional DPC strategy compared to the DPC-FPI strategy.
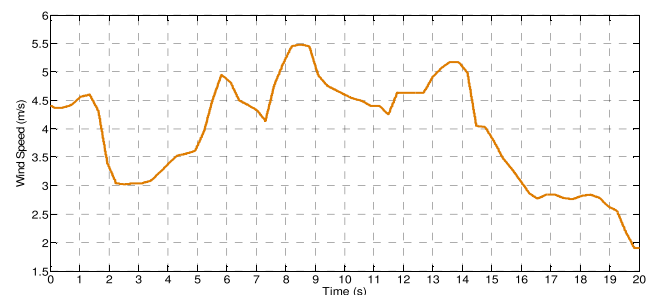
FIGURE 13. WS profile.

The currents are represented in Figures 17 and 18 for the two controls, where it is noted that the currents change according to the change in WS, as they decrease with decreasing WS and increase with increasing WS. The shape of the currents is sinusoidal, with the proposed DPC-FPI strategy having an advantage in terms of quality and ripples compared to the traditional DPC technique. The THD value of current for the two controls is represented in Figure 19, where the THD value for the traditional strategy was
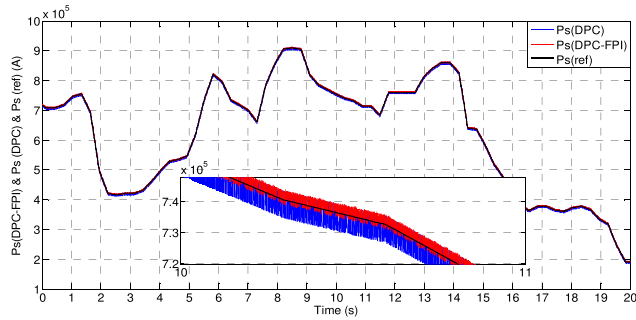
FIGURE 14. *Ps* of DPC-FPI and DPC.
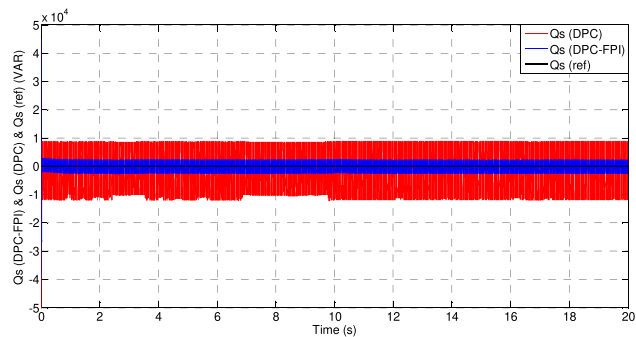
FIGURE 15. *Qs* of DPC-FPI and DPC.

FIGURE 16. Torque.

a) DPC-FPI
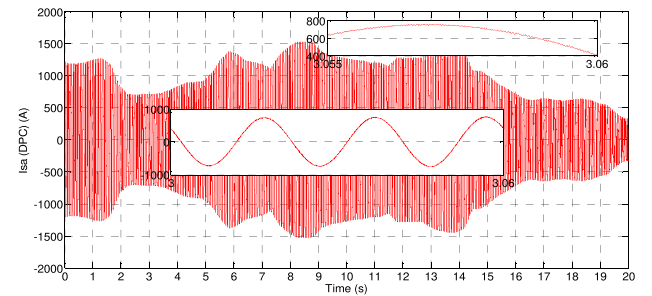
b)DPC

FIGURE 17. Current (Isa).

estimated at 0.36% and 0.11% for the proposed strategy. So, the proposed strategy significantly reduced the THD value, which is a good thing and indicates that the quality of the current is better if the proposed strategy is used compared to the traditional strategy. Therefore, the percentage of reduction in the THD value is 69.44% compared to the traditional strategy, as this percentage indicates that the current ripples are very low in the proposed strategy compared to the traditional strategy. On the other hand, Figure 19 shows that the amplitude value of the fundamental (50 Hz) of current signal is slightly high in the traditional strategy compared to the proposed strategy, as the amplitude value was 2514 A and 2513 A for both the traditional and proposed strategy, respectively. So, the amplitude of the fundamental signal represents the negativity of the proposed strategy in this test, which is undesirable. Smart strategies such as genetic algorithms can be used to overcome this problem.

In Table 3, the change in the value of THD of current in the two tests is shown, as it explains the extent to which the value of THD is affected by the change in the shape of the wind speed. From this table, it can be said that changing the shape of the wind speed affects the THD value of a stream, as it is noted that the THD value for the two controls was high in the first test compared to the second test. This increase was estimated at 2.7% and 15.38% for both the traditional and proposed strategies, respectively. So the proposed strategy provided a greater rate of increase than the traditional strategy, which indicates that it is affected by

the change in the shape of the wind speed more than the traditional strategy, which is undesirable.

TABLE 3. Values and percentages of change in the value of THD of current in the two tests.

	THD value of current	
	DPC-PI	**DPC-FPI**
First test	0.37%	0.13%
Second test	0.36%	0.11%
Ratios	2.70%	15.38%

The reduction percentages for this test are represented in Table 4, where the values and reduction percentages are given for response time, ripples, SSE, and overshoot of *Ps* and *Qs*. The calculated ratios indicate the distinctive performance of the proposed DPC-FPI strategy compared to the traditional DPC strategy in terms of reducing energy ripples, overshoot and SSE of *Ps* and *Qs*. The proposed DPC-FPI strategy has a negative aspect, which is that it

a) DPC-FPI

b)DPC
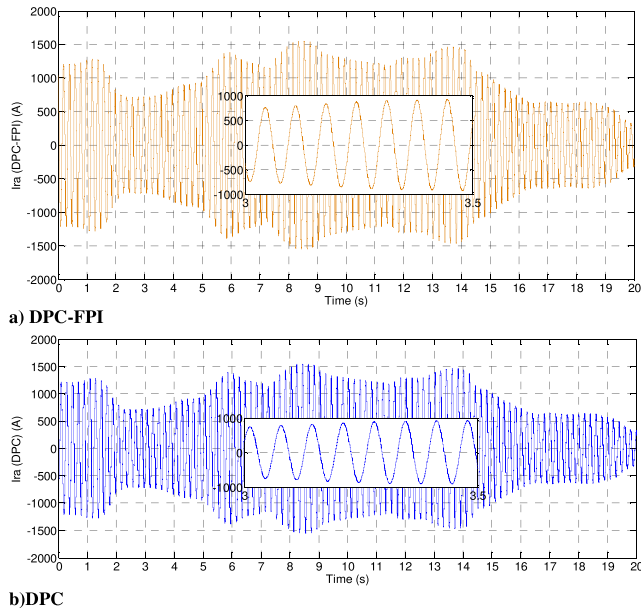
FIGURE 18. Current (*I*ra).

a)DPC-PI

b)DPC-FPI
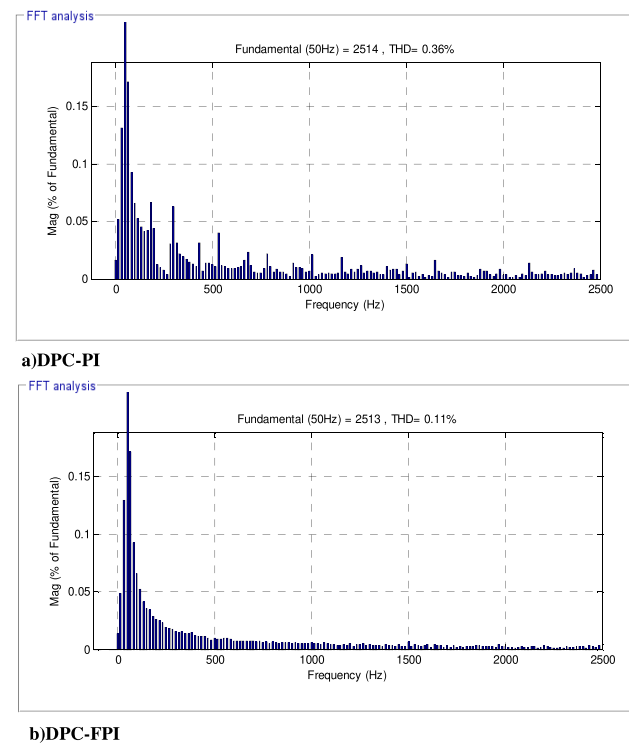
FIGURE 19. THD value of current (Test_2).

provides an unsatisfactory response time to power compared to the traditional DPC strategy, as the traditional DPC strategy reduced the response time by 97.04% and 55.97% for both reactive and active power, respectively, compared to the proposed DPC-FPI strategy, which is unsatisfactory. This can be overcome by using intelligent strategies such as genetic algorithm in determining gain values.

TABLE 4. Value and improvement ratios of overshoot, response time, SSE and power ripples of both techniques in the second test.

		Ps (W)	*Qs* (VAR)
DPC	Ripples	10050	19200
	Overshoot	3500	608
	SSE	11000	12060
	Response time	0.59ms	0.035ms
DPC-FPI	Ripples	460	4026
	Overshoot	320	98
	SSE	1560	3045
	Response time	1.34ms	1.183ms
Improvement Ratios	Ripples	95.42%	79.03%
	Overshoot	90.86%	83.88%
	SSE	85.82%	74.75%
	Response time	-55.97%	-97.04%

In Tables 5, 6, 7, and 8 a comparison with other works is made in terms of ripple reduction ratios, overshoot, and SSE of *Ps* and *Qs*. In addition to the value of the response time for the capabilities provided. These tables give a clear picture of the superiority of the proposed DPC-FPI strategy over several different strategies, as it provided better reduction ratios, which indicates outstanding performance and high efficiency in improving the system characteristics.

TABLE 5. Comparison in terms of power ripples minimization rates.

References		Ratios	
		Qs (VAR)	*Ps (W)*
[31]	**Intelligent control**	35%	36%
[26]		36.93%	22.95%
[32]	**BC technique**	46.93%	28.57%
[28]		46.68%	47.50%
[33]	**STA**	22.66%	21.75%
	Modified STA	21.23%	19.11%
[27]		50%	44.50%
[30]		37.48%	57.09%
[34]		47.99%	65.07%
[3]		43.07%	33%
Proposed technique	**First test**	37.51%	58.60%
	Third test	79.03%	95.42%

TABLE 6. Comparison in terms of SSE minimization rates.

References		SSE ratios	
		Qs (VAR)	*Ps (W)*
[26]		36.93%	35%
[32]		42.14%	47.57%
[28]		52.22%	56.52%
[31]		35.48%	62%
[27]		53.25%	74.41%
[30]		46.86%	63.96%
[23]		80%	77.27
Proposed technique	**Test_1**	84.13%	52.21%
	Test_2	74.75%	85.82%

VI. EXPERIMENTAL RESULTS
A. DSPACE DS1104 RESEARCH AND DEVELOPMENT CONTROLLER BOARD
Rapid control prototyping is enabled by the DS1104 R&D Controller Board [53], which converts a personal computer

TABLE 7. Comparison in terms of overshoot minimization rates.

References	Overshoot ratios	
	Qs (VAR)	Ps (W)
[32]	60.93%	67.74%
[23]	91.72%	71.33%
[35]	16.59%	7.23%
[36]	60.93%	67.74%
[31]	37.42%	80%
[27]	49.32%	20.10%
Proposed technique	83.88%	90.86%

TABLE 8. Comparison in terms of response time for Ps and Qs.

References		Time Response (ms)	
		Ps (W)	Qs (VAR)
[37]		-	28ms
[17]		33.8ms	34.5ms
[38]		15ms	80ms
[39]		32ms	-
[40]	**DPC**	17ms	18ms
	Nonlinear DPC method	9ms	5ms
Proposed technique	**Test_1**	1.70ms	1.85ms
	Test_2	1.34ms	1.183ms

TABLE 9. A comparison between existing works and the proposed work in terms of THD value of current.

Techniques	THD (%)	References
DPC-HOSMC	1.66	[41]
FSMC	3.1	[42]
Intelligent DTC	4.80	[43]
SOSMC	3.13	[44]
FOC	3.70	[45]
ISMC	0.88	[37]
Virtual flux DPC	4.88	[46]
DTC with intelligent control	7.19	[47]
Multi-resonant-based SMC	3.2	[48]
Predictive DTC	2.15	[49]
Fuzzy DTC	2.04	[50]
DPC with neuro-fuzzy algorithm	2.72	[51]
DTC-SOCSM	0.98	[52]
Proposed technique	Test_1	0.13
	Test_2	0.11

FIGURE 20. Dspace DS1104 research and development controller board.
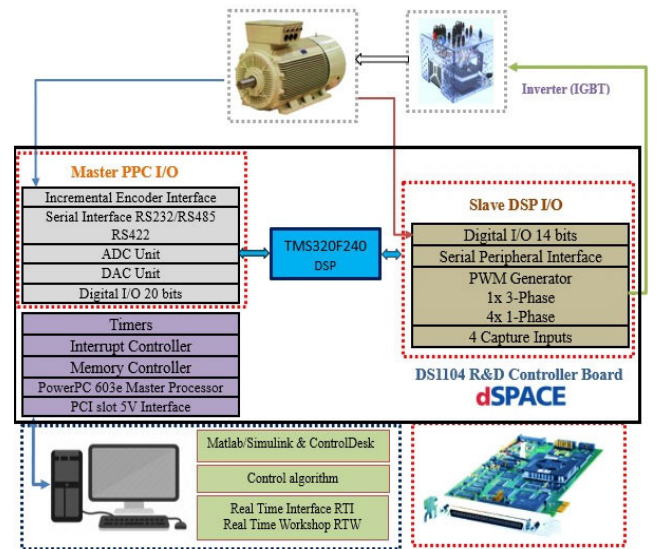
FIGURE 21. Implementation structure of DPC-FPI strategy.
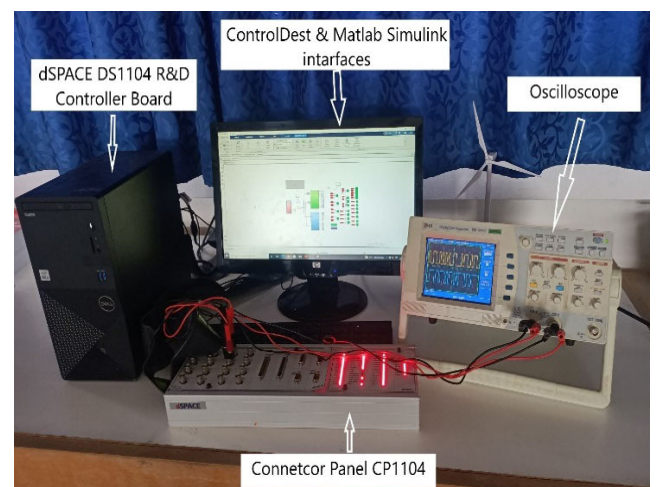
FIGURE 22. Hardware-software experimental implementation of DPC-FPI strategy.

(PC) into a development system. Almost any PC with a 5V free PCI or PCIe slot may install the board. It is a system having a real-time processor that is inexpensive (see Figure 18). The dSPACE controller and MATLAB/Simulink software together provide an effective, powerful, and high development environment [54]. The DS1104 R&D controller board's Real-Time Interface (RTI) allows the function models to be readily run on it. It is simple and graphic to configure all inputs and outputs (I/O). A Simulink block diagram will be expanded to include all control system blocks, and Simulink® Coder TM will create the model code. The model code will be produced using Simulink® Coder TM (formerly Real-Time Workshop) using RTI. The control system's outputs and inputs can be graphically configured using the Control Desk software. Automatic compilation, download, and startup of the real-time model (rtModel) will
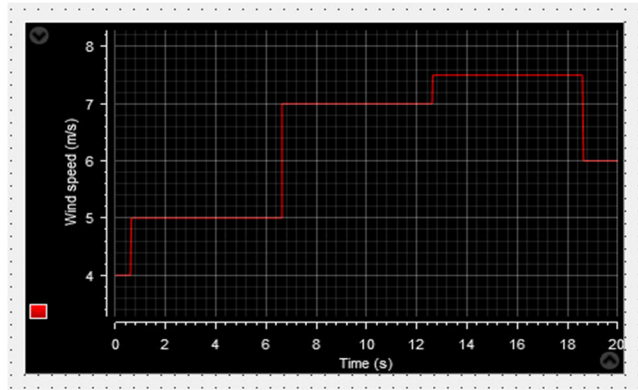
a) WS profile (Steps)
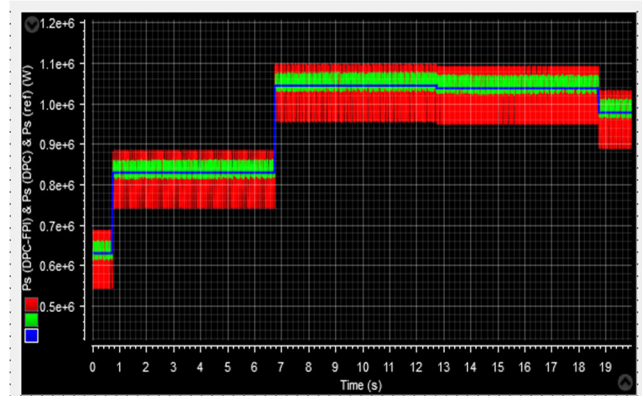
b) Ps (DPC–FPI and DPC)
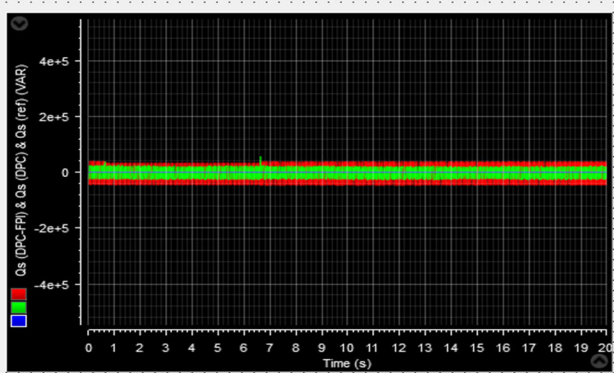
c) Qs (DPC–FPI and DPC)
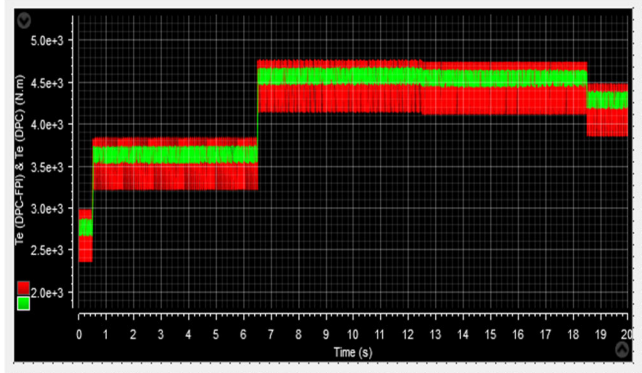
d) Torque (DPC–FPI and DPC)
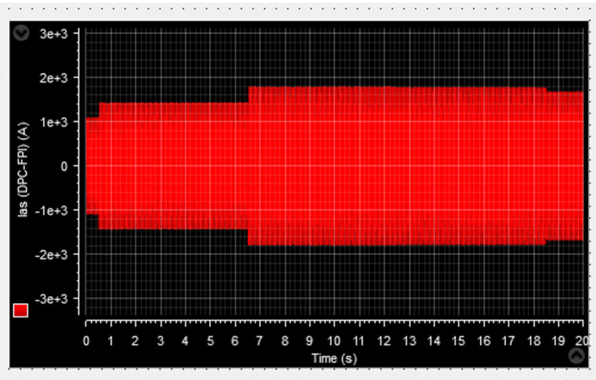
e) Stator current (I_{sa}) of DPC-FPI
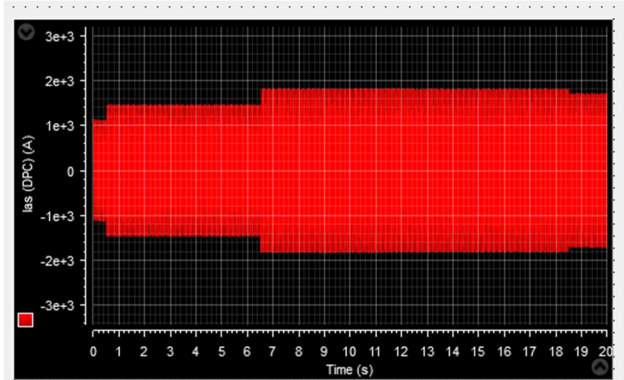
f) Stator current (I_{sa}) of DPC
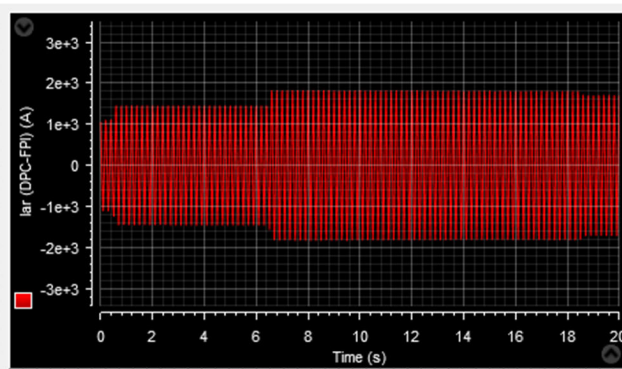
g) Rotor current (I_{ra}) of DPC-FPI
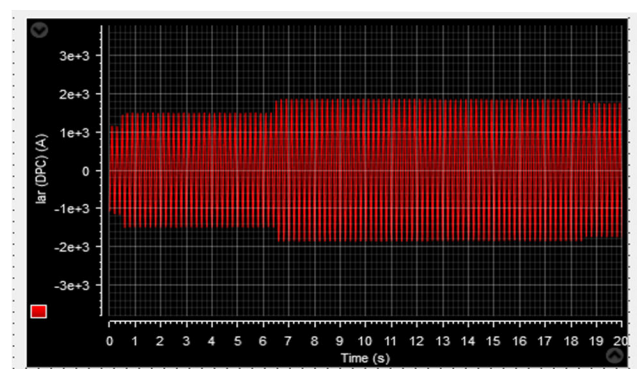
h) Rotor current (I_{ra}) of DPC.

FIGURE 23. Experimental results in the steps wind speed test.
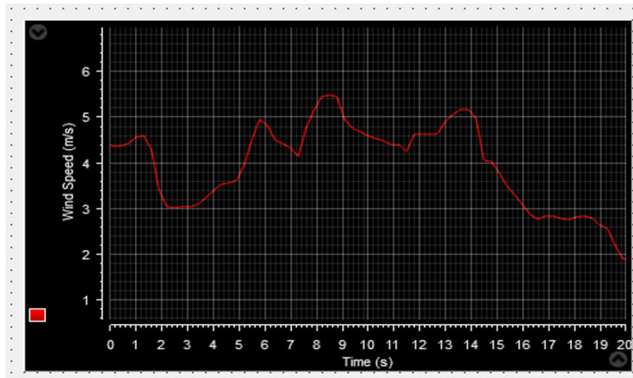
a) WS profile
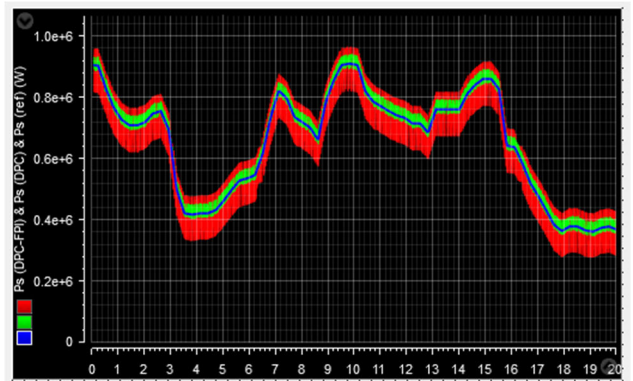
b) *Ps* of DPC-FPI and DPC
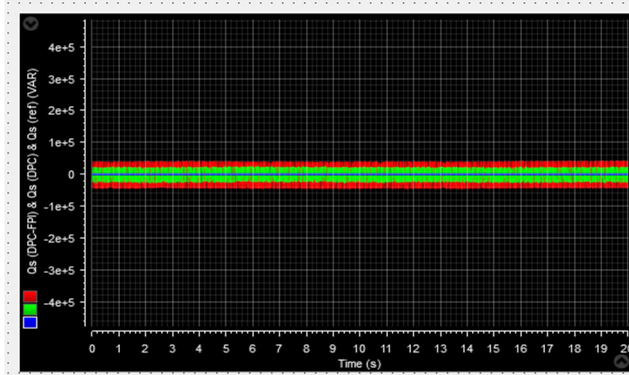
c) *Qs* of DPC-FPI and DPC
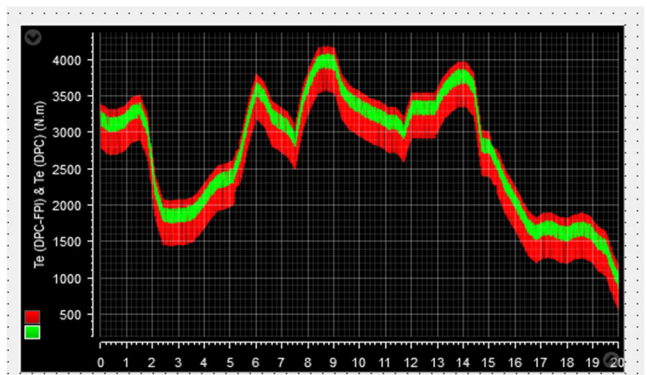
d) Torque of DPC-FPI and DPC
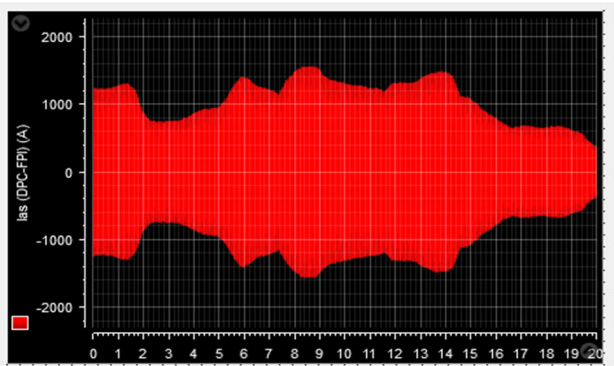
e) Stator current (I_{sa}) of DPC-FPI
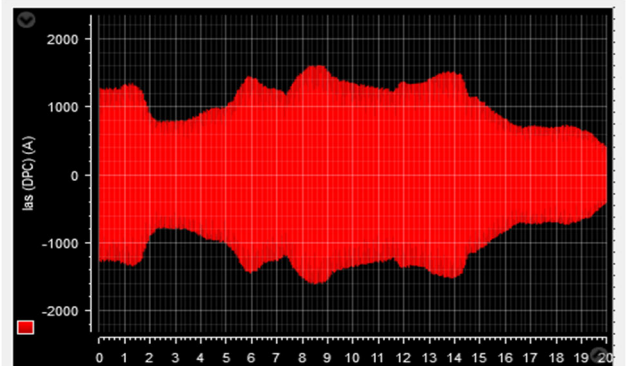
f) Stator current (I_{sa}) of DPC
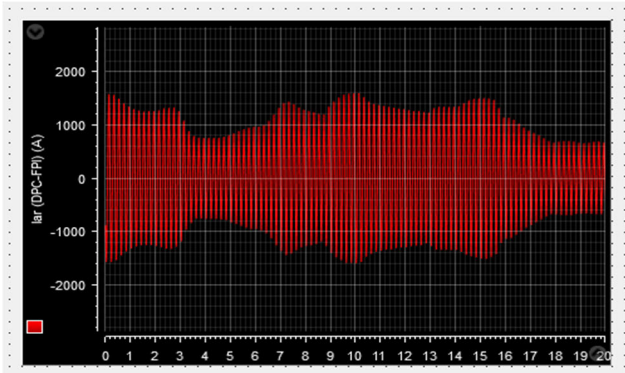
g) Rotor current (I_{ra}) of DPC-FPI
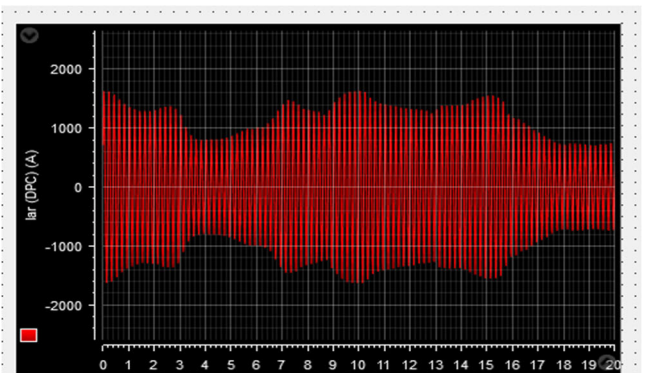
h) Rotor current (I_{ra}) of DPC

FIGURE 24. Experimental results in the variable WS test.

take place. This fact cuts the cost and implementation time to a minimum. In addition, it increases the performance and the productivity [54], [55].

The hardware and software needed to build and validate the suggested control technique are shown in Figure 19. The DS1104 Controller board's technical specifications are also included. This board was used to experimentally validate the suggested DPC-FPI technique. This embedded system card includes a Power PC MPC 8240 core processor, a 64-bit floating point processor operating at 250 MHz, a 100 MHz bus, a primary PPC I/O subsystem, and a secondary DSP I/O [56], [57]. This embedded system sends the necessary signals to the IGBT inverter in real time, as shown in Figure 19 [54].

Three parts make up the dSPACE Package, which is used for experimental validation [55]:

- The dSPACE DS1104 R&D controller board installed on the PC.
- The connector panel DS1104 for connecting signal lines to the dSPACE DS1104 R&D controller board.
- The software tools for operating the embedded card through the MATLAB/Simulink environment block diagram.

In Figure 20, the hardware implementation of the WE conversion system based on a DFIG with two scenarios—step wind profile and changeable wind profile—is depicted. Utilizing a dSPACE DS1104 R&D Controller card with RTI block set libraries and the MATLAB 2021b environment, this experimental implementation and validation was carried out. All measurements requested by the developed strategy utilizing the real-time workshop (RTW) tool and the real-time interface (RTI) are collected from the WE system by the DS1104 controller board. The system is effectively controlled using the dSPACE DS1104 controller.

PWM signals are produced by the Texas Instruments TMS320F240 DSP, the secondary DSP, and the simulated controller model is computed by the Power PC (PPC 603e core). The digital oscilloscope displays the PWM signals that are taken from the secondary Inputs/Outputs PWM connector on the connection panel CP1104 connector panel (see Figure 20) [53].

The results of the hardware simulation of the embedded wind conversion system with the suggested DPC-FPI strategy are shown in the figures below, which were made using the graphical interface of the dSPACE 1104 Real-Time Interface (RTI) under Control Desk (version 7.6).

B. REAL TIME EXPERIMENTAL RESULTS

The experimental results obtained are represented in Figures 20 and 22, where two forms of WS were used in order to study the efficiency of the proposed DPC-FPI strategy compared to the traditional DPC strategy. the experimental results obtained confirm the simulation results listed above, as it is noted from Figures 21 and 22 that the powers follow the references well, with fewer ripples in the case of the suggested DPC-FPI strategy compared to traditional DPC

technique. moreover, experimentally, active power is related to WS and reactive power is not related to WS, which are the same observations found in the simulation results. the torque takes the form of active power in both cases of WS, where its value increases with increasing WS and vice versa. also, it is noted that the proposed strategy significantly reduced momentum ripples, which is desirable. Regarding currents, they take the form of active power changes with a sinusoidal shape. It is noted that the value of the currents is affected by the change in the shape of the WS to a large extent, with better quality in the case of the proposed DPC-FPI strategy compared to traditional DPC technique.

These experimental results give a clear picture of the superiority of the proposed DPC-FPI strategy, especially the FPI controller, compared to the traditional controller. the experimental results refute the validity of the results obtained from the MATLAB environment, and therefore this strategy can be adopted in the future in the field of renewable energies.

VII. CONCLUSION

An experimental work was presented dealing with the application of a new linear controller to overcome the problems of the DPC technique of DFIG. The proposed strategy was first implemented in the MATLAB environment, where the necessary numerical and graphical results were extracted to prove the superiority of the proposed DPC-FPI strategy compared to the traditional DPC strategy. In addition to achieving comparison with other works in terms of reducing ripple rates, response time, overshoot, and SSE of DFIG power. The experimental results obtained using Dspace 1104 prove the validity of the experimental results and the effective performance of the proposed DPC-FPI technique. The results achieved from this work can be summarized in the following points:

- Reducing energy waves.
- Significantly overcome the problems of the traditional DPC strategy.
- Increasing the robustness of the system while improving the quality of the current compared to the traditional strategy.
- The FPI controller is more efficient than the traditional controller.

In the future, other strategies will be implemented on the energy system based on DFIG, where hybrid nonlinear strategies will be used in order to significantly increase performance and reduce energy ripples.

REFERENCES

[1] B. Hu, H. Nian, H. Li, L. Chen, S. Sahoo, and F. Blaabjerg, "Impedance reshaping band coupling and broadband passivity enhancement for DFIG system," *IEEE Trans. Power Electron.*, vol. 38, no. 8, pp. 9436–9447, Aug. 2023, doi: 10.1109/TPEL.2023.3270364.

[2] K.-J. Du, X.-P. Ma, Z.-X. Zheng, C.-S. Li, W.-X. Hu, and K.-S. Dong, "LVRT capability improvement of DFIG-based wind turbines with a modified bridge-resistive-type SFCL," *IEEE Trans. Appl. Supercond.*, vol. 31, no. 8, pp. 1–5, Nov. 2021, doi: 10.1109/TASC.2021.3091114.

[3] H. Benbouhenni, N. Bizon, I. Colak, M. I. Mosaad, and M. Yessef, "Direct active and reactive powers control of double-powered asynchronous generators in multi-rotor wind power systems using modified synergetic control," *Energy Rep.*, vol. 10, pp. 4286–4301, Nov. 2023, doi: 10.1016/j.egyr.2023.10.085.

[4] W. Ullah, F. Khan, S. Hussain, M. Yousaf, and S. Akbar, "A novel dual port dual rotor wound field flux switching generator with uniform and non-uniform rotor poles for counter-rotating wind power generation," *IEEE Trans. Energy Convers.*, vol. 38, no. 4, pp. 2420–2433, Dec. 2023, doi: 10.1109/TEC.2023.3272520.

[5] O. Beik and A. S. Al-Adsani, "Active and passive control of a dual rotor wind turbine generator for DC grids," *IEEE Access*, vol. 9, pp. 1987–1995, 2021, doi: 10.1109/ACCESS.2020.3047267.

[6] W. Ullah, F. Khan, and S. Hussain, "A novel dual rotor permanent magnet flux switching generator for counter rotating wind turbine applications," *IEEE Access*, vol. 10, pp. 16456–16467, 2022, doi: 10.1109/ACCESS.2022.3149895.

[7] W. Ullah, F. Khan, and S. Hussain, "A comparative study of dual stator with novel dual rotor permanent magnet flux switching generator for counter rotating wind turbine applications," *IEEE Access*, vol. 10, pp. 8243–8261, 2022, doi: 10.1109/ACCESS.2022.3143166.

[8] S. Kadi, K. Imarazene, E. M. Berkouk, H. Benbouhenni, and E. Abdelkarim, "A direct vector control based on modified SMC theory to control the double-powered induction generator-based variable-speed contra-rotating wind turbine systems," *Energy Rep.*, vol. 8, pp. 15057–15066, Nov. 2022, doi: 10.1016/j.egyr.2022.11.052.

[9] W. Ullah, F. Khan, U. B. Akuru, S. Hussain, M. Yousaf, and S. Akbar, "A novel dual electrical and dual mechanical wound field flux switching generator for co-rotating and counter-rotating wind turbine applications," *IEEE Trans. Ind. Appl.*, pp. 1–12, Sep. 2023. [Online]. Available: https://ieeexplore.ieee.org/document/10247651, doi: 10.1109/TIA.2023.3314591.

[10] J. Mohammadi, S. Vaez-Zadeh, S. Afsharnia, and E. Daryabeigi, "A combined vector and direct power control for DFIG-based wind turbines," *IEEE Trans. Sustain. Energy*, vol. 5, no. 3, pp. 767–775, Jul. 2014, doi: 10.1109/TSTE.2014.2301675.

[11] H. Benbouhenni, Z. Boudjema, N. Bizon, P. Thounthong, and N. Takorabet, "Direct power control based on modified sliding mode controller for a variable-speed multi-rotor wind turbine system using PWM strategy," *Energies*, vol. 15, no. 10, p. 3689, May 2022, doi: 10.3390/en15103689.

[12] H. Benbouhenni, "Application of DPC and DPC-GA to the dual-rotor wind turbine system with DFIG," *IAES Int. J. Robot. Autom. (IJRA)*, vol. 10, no. 3, p. 224, Sep. 2021, doi: 10.11591/ijra.v10i3.pp224-234.

[13] H. Chojaa, A. Derouich, S. E. Chehaidia, O. Zamzoum, M. Taoussi, H. Benbouhenni, and S. Mahfoud, "Enhancement of direct power control by using artificial neural network for a doubly fed induction generator-based WECS: An experimental validation," *Electronics*, vol. 11, no. 24, p. 4106, Dec. 2022, doi: 10.3390/electronics11244106.

[14] I. Boussaid, A. Harrouz, and P. Wira, "Advanced control of doubly fed induction generator for wind power systems: Optimal control of power using PSO algorithm," *Appl. Mech. Mater.*, vol. 905, pp. 29–42, Feb. 2022, doi: 10.4028/p-20n6a9.

[15] K. F. Sayeh, S. Tamalouzt, and Y. Sahri, "Improvement of power quality in WT-DFIG systems using novel direct power control based on fuzzy logic control under randomness conditions," *Int. J. Model. Simul.*, pp. 1–13, Oct. 2023. [Online]. Available: https://www.tandfonline.com/doi/full/10.1080/02286203.2023.2270757?scroll=top&needAccess=true, doi: 10.1080/02286203.2023.2270757.

[16] H. Benbouhenni and N. Bizon, "Terminal synergetic control for direct active and reactive powers in asynchronous generator-based dual-rotor wind power systems," *Electronics*, vol. 10, no. 16, p. 1880, Aug. 2021, doi: 10.3390/electronics10161880.

[17] P. Xiong and D. Sun, "Backstepping-based DPC strategy of a wind turbine-driven DFIG under normal and harmonic grid voltage," *IEEE Trans. Power Electron.*, vol. 31, no. 6, pp. 4216–4225, Jun. 2016, doi: 10.1109/TPEL.2015.2477442.

[18] A. Almakki, A. Mazalov, H. Benbouhenni, and N. Bizon, "Comparison of two fractional-order high-order SMC techniques for DFIG-based wind turbines: Theory and simulation results," *ECTI Trans. Electr. Eng., Electron., Commun.*, vol. 21, no. 2, Jun. 2023, Art. no. 249817, doi: 10.37936/ecti-eec.2023212.249817.

[19] L. Shang and J. Hu, "Sliding-mode-based direct power control of grid-connected wind-turbine-driven doubly fed induction generators under unbalanced grid voltage conditions," *IEEE Trans. Energy Convers.*, vol. 27, no. 2, pp. 362–373, Jun. 2012, doi: 10.1109/TEC.2011.2180389.

[20] S. Kadi, H. Benbouhenni, E. Abdelkarim, K. Imarazene, and E. M. Berkouk, "Implementation of third-order sliding mode for power control and maximum power point tracking in DFIG-based wind energy systems," *Energy Rep.*, vol. 10, pp. 3561–3579, Nov. 2023, doi: 10.1016/j.egyr.2023.09.187.

[21] H. Benbouhenni, F. Mehedi, and L. Soufiane, "New direct power synergetic-SMC technique based PWM for DFIG integrated to a variable speed dual-rotor wind power," *Automatika*, vol. 63, no. 4, pp. 718–731, Dec. 2022, doi: 10.1080/00051144.2022.2065801.

[22] F. Echiheb, Y. Ihedrane, B. Bossoufi, M. Bouderbala, S. Motahhir, M. Masud, S. Aljahdali, and M. ElGhamrasni, "Robust sliding-backstepping mode control of a wind system based on the DFIG generator," *Sci. Rep.*, vol. 12, no. 1, p. 11782, Jul. 2022, doi: 10.1038/s41598-022-15960-7.

[23] H. Benbouhenni, I. Colak, N. Bizon, and E. Abdelkarim, "Fractional-order neural control of a DFIG supplied by a two-level PWM inverter for dual-rotor wind turbine system," *Meas. Control*, Oct. 2023. [Online]. Available: https://journals.sagepub.com/doi/epub/10.1177/00202940231201375

[24] H. Benbouhenni, N. Bizon, M. I. Mosaad, I. Colak, A. B. Djilali, and H. Gasmi, "Enhancement of the power quality of DFIG-based dual-rotor wind turbine systems using fractional order fuzzy controller," *Expert Syst. Appl.*, vol. 238, Mar. 2024, Art. no. 121695, doi: 10.1016/j.eswa.2023.121695.

[25] H. Benbouhenni, I. Colak, and N. Bizon, "Application of genetic algorithm and terminal sliding surface to improve the effectiveness of the proportional–integral controller for the direct power control of the induction generator power system," *Eng. Appl. Artif. Intell.*, vol. 125, Oct. 2023, Art. no. 106681, doi: 10.1016/j.engappai.2023.106681.

[26] H. Benbouhenni, H. Gasmi, I. Colak, N. Bizon, and P. Thounthong, "Synergetic-PI controller based on genetic algorithm for DPC-PWM strategy of a multi-rotor wind power system," *Sci. Rep.*, vol. 13, no. 1, p. 13570, Aug. 2023, doi: 10.1038/s41598-023-40870-7.

[27] H. Benbouhenni, D. Zellouma, N. Bizon, and I. Colak, "A new PI(1+PI) controller to mitigate power ripples of a variable-speed dual-rotor wind power system using direct power control," *Energy Rep.*, vol. 10, pp. 3580–3598, Nov. 2023, doi: 10.1016/j.egyr.2023.10.007.

[28] H. Benbouhenni, E. Bounadja, H. Gasmi, N. Bizon, and I. Colak, "A new PD(1+PI) direct power controller for the variable-speed multi-rotor wind power system driven doubly-fed asynchronous generator," *Energy Rep.*, vol. 8, pp. 15584–15594, Nov. 2022, doi: 10.1016/j.egyr.2022.11.136.

[29] H. Benbouhenni, M. I. Mosaad, I. Colak, N. Bizon, H. Gasmi, M. Aljohani, and E. Abdelkarim, "Fractional-order synergetic control of the asynchronous generator-based variable-speed multi-rotor wind power systems," *IEEE Access*, vol. 11, pp. 133490–133508, 2023, doi: 10.1109/ACCESS.2023.3335902.

[30] H. Benbouhenni, I. Colak, N. Bizon, A. G. Mazare, and P. Thounthong, "Direct vector control using feedback PI controllers of a DPAG supplied by a two-level PWM inverter for a multi-rotor wind turbine system," *Arabian J. Sci. Eng.*, vol. 48, no. 11, pp. 15177–15193, Nov. 2023, doi: 10.1007/s13369-023-08035-w.

[31] H. Benbouhenni, "Intelligent control scheme of asynchronous generator-based dual-rotor wind power system under different working conditions," *Majlesi J. Energy Manag.*, vol. 11, no. 3, pp. 8–15, 2022. [Online]. Available: https://em.majlesi.info/index.php/em/article/view/494

[32] H. Benbouhenni, "Backstepping control for multi-rotor wind power systems," *Majlesi J. Energy Manag.*, vol. 11, no. 4, pp. 8–15, 2022. [Online]. Available: https://em.majlesi.info/index.php/em/article/view/493

[33] K. Xiahou, M. S. Li, Y. Liu, and Q. H. Wu, "Sensor fault tolerance enhancement of DFIG-WTs via perturbation observer-based DPC and two-stage Kalman filters," *IEEE Trans. Energy Convers.*, vol. 33, no. 2, pp. 483–495, Jun. 2018, doi: 10.1109/TEC.2017.2771250.

[34] H. Benbouhenni, N. Bizon, P. Thounthong, I. Colak, and P. Mungporn, "A new integral-synergetic controller for direct reactive and active powers control of a dual-rotor wind system," *Meas. Control*, Sep. 2023. [Online]. Available: https://journals.sagepub.com/doi/epub/10.1177/00202940231201375, doi: 10.1177/00202940231195117.

[35] H. Gasmi, H. Benbouhenni, S. Mendaci, and I. Colak, "A new scheme of the fractional-order super twisting algorithm for asynchronous generator-based wind turbine," *Energy Rep.*, vol. 9, pp. 6311–6327, Dec. 2023, doi: 10.1016/j.egyr.2023.05.267.

[36] H. Benbouhenni, "Comparative study of sliding mode control with synergetic control for rotor side inverter of the DFIG for multi-rotor wind power systems," *Majlesi J. Mechatron. Syst.*, vol. 11, no. 2, pp. 29–37, 2023. [Online]. Available: https://ms.majlesi.info/index.php/ms/article/view/532

[37] H. Chojaa, A. Derouich, S. E. Chehaidia, O. Zamzoum, M. Taoussi, and H. Elouatouat, "Integral sliding mode control for DFIG based WECS with MPPT based on artificial neural network under a real wind profile," *Energy Rep.*, vol. 7, pp. 4809–4824, Nov. 2021, doi: 10.1016/j.egyr.2021.07.066.

[38] H. E. Alami, B. Bossoufi, S. Motahhir, E. H. Alkhammash, M. Masud, M. Karim, M. Taoussi, M. Bouderbala, M. Lamnadi, and M. El Mahfoud, "FPGA in the loop implementation for observer sliding mode control of DFIG-generators for wind turbines," *Electronics*, vol. 11, no. 1, p. 116, Dec. 2021, doi: 10.3390/electronics11010116.

[39] B. Bossoufi, M. Karim, A. Lagrioui, and M. Taoussi, "FPGA-based implementation nonlinear backstepping control of a PMSM drive," *Int. J. Power Electron. Drive Syst. (IJPEDS)*, vol. 4, no. 1, pp. 12–23, Dec. 2014.

[40] Y. Ibrahim, "Neuro-second order sliding mode control of a DFIG based wind turbine system," *J. Electr. Electron. Eng.*, vol. 13, no. 1, pp. 63–68, 2020.

[41] I. Yaichi, A. Semmah, P. Wira, and Y. Djeriri, "Super-twisting sliding mode control of a doubly-fed induction generator based on the SVM strategy," *Periodica Polytechnica Electr. Eng. Comput. Sci.*, vol. 63, no. 3, pp. 178–190, Jun. 2019, doi: 10.3311/PPee.13726.

[42] M. Benmeziane, S. Zebirate, A. Chaker, and Z. Boudjema, "Fuzzy sliding mode control of doubly-fed induction generator driven by wind turbine," *Int. J. Power Electron. Drive Syst. (IJPEDS)*, vol. 10, no. 3, p. 1592, Sep. 2019, doi: 10.11591/ijpeds.v10.i3.pp1592-1602.

[43] S. Mahfoud, A. Derouich, N. EL Ouanjli, M. EL Mahfoud, and M. Taoussi, "A new strategy-based PID controller optimized by genetic algorithm for DTC of the doubly fed induction motor," *Systems*, vol. 9, no. 2, p. 37, May 2021, doi: 10.3390/systems9020037.

[44] A. Yahdou, "Second order sliding mode control of a dual-rotor wind turbine system by employing a matrix converter," *J. Electr. Eng.*, vol. 16, no. 3, pp. 1–11, 2016.

[45] F. Amrane, A. Chaiba, B. Babes, and S. Mekhilef, "Design and implementation of high performance field oriented control for grid-connected doubly fed induction generator via hysteresis rotor current controller," *Rev. Roum. Sci. Techn.-Electrotechn. Et Energ*, vol. 61, no. 4, pp. 319–324, 2016.

[46] N. A. Yusoff, "A Concept of virtual-flux direct power control of three-phase AC-DC converter," *Int. J. Power Electron. Drive Syst.*, vol. 8, no. 4, pp. 1776–1784, 2017, doi: 10.11591/ijpeds.v8i4.pp1776-1784.

[47] S. Mahfoud, A. Derouich, A. Iqbal, and N. El Ouanjli, "ANT-colony optimization-direct torque control for a doubly fed induction motor : An experimental validation," *Energy Rep.*, vol. 8, pp. 81–98, Nov. 2022, doi: 10.1016/j.egyr.2021.11.239.

[48] Y. Quan, L. Hang, Y. He, and Y. Zhang, "Multi-resonant-based sliding mode control of DFIG-based wind system under unbalanced and harmonic network conditions," *Appl. Sci.*, vol. 9, no. 6, p. 1124, Mar. 2019, doi: 10.3390/app9061124.

[49] M. A. Mossa, H. Echeikh, and A. Iqbal, "Enhanced control technique for a sensor-less wind driven doubly fed induction generator for energy conversion purpose," *Energy Rep.*, vol. 7, pp. 5815–5833, Nov. 2021, doi: 10.1016/j.egyr.2021.08.183.

[50] W. Ayrir, M. Ourahou, B. El Hassouni, and A. Haddi, "Direct torque control improvement of a variable speed DFIG based on a fuzzy inference system," *Math. Comput. Simul.*, vol. 167, pp. 308–324, Jan. 2020, doi: 10.1016/j.matcom.2018.05.014.

[51] Y. Sahri, S. Tamalouzt, F. Hamoudi, S. L. Belaid, M. Bajaj, M. M. Alharthi, M. S. Alzaidi, and S. S. M. Ghoneim, "New intelligent direct power control of DFIG-based wind conversion system by using machine learning under variations of all operating and compensation modes," *Energy Rep.*, vol. 7, pp. 6394–6412, Nov. 2021, doi: 10.1016/j.egyr.2021.09.075.

[52] Z. Boudjema, R. Taleb, Y. Djeriri, and A. Yahdou, "A novel direct torque control using second order continuous sliding mode of a doubly fed induction generator for a wind energy conversion system," *TURKISH J. Electr. Eng. Comput. Sci.*, vol. 25, no. 2, pp. 965–975, 2017, doi: 10.3906/elk-1510-89.

[53] *Artisan Technology Group (ArtisanTG)*. Accessed: Dec. 1, 2023. [Online]. Available: https://www.artisantg.com/TestMeasurement/89132-3/dSPACE-DS1104-Research-and-Development-Controller-Board

[54] S. Mensou, A. Essadki, T. Nasser, B. B. Idrissi, and L. Ben Tarla, "Dspace DS1104 implementation of a robust nonlinear controller applied for DFIG driven by wind turbine," *Renew. Energy*, vol. 147, pp. 1759–1771, Mar. 2020, doi: 10.1016/j.renene.2019.09.042.

[55] A. Beddar, H. Bouzekri, B. Babes, and H. Afghoul, "Experimental enhancement of fuzzy fractional order PI+I controller of grid connected variable speed wind energy conversion system," *Energy Convers. Manage.*, vol. 123, pp. 569–580, Sep. 2016, doi: 10.1016/j.enconman.2016.06.070.

[56] N. V. Naik and S. P. Singh, "A comparative analytical performance of F2DTC and PIDTC of induction motor using DSPACE-1104," *IEEE Trans. Ind. Electron.*, vol. 62, no. 12, pp. 7350–7359, Dec. 2015, doi: 10.1109/TIE.2015.2463758.

[57] Z. Boudjema, "DSPACE implementation of a neural SVPWM technique for a two level voltage source inverter," *Iran. J. Electr. Electron. Eng.*, vol. 17, no. 3, pp. 1–9, 2021.

MOURAD YESSEF was born in Taounate, Morocco. He received the master's degree in science and technology titled microelectronic from the Faculty of Sciences, Sidi Mohamed Ben Abdellah University, Fes, Morocco, where he is currently pursuing the Ph.D. degree in electrical engineering. His main research interests include renewable energy, smart grid, artificial intelligence, embedded systems, control systems, and power electronics.

HABIB BENBOUHENNI was born in Chlef, Algeria. He received the M.A. degree in automatic and informatique industrial, in 2017. He is currently pursuing the Ph.D. degree with the Department of Electrical Engineering, ENPO-MA, Oran, Algeria. He is also a Professor with Nişantaşı University, Turkey. He is an editor of seven books and more than 180 articles in scientific fields related to electrical engineering. His research interest includes the application of robust control in the wind turbine power systems.

MOHAMMED TAOUSSI was born in Fez, Morocco. He received the master's degree in industrial electronics from the Faculty of Sciences, Fes, in 2013, and the Ph.D. degree in electrical engineering from the Faculty of Sciences, University Sidi Mohammed Ben Abdellah, Morocco.

He is currently a Professor with University Sidi Mohammed Ben Abdellah. His research interests include static converters, electrical motor drives, and power electronics, smart grid, renewable energy, and artificial intelligence.

AHMED LAGRIOUI received the Ph.D. degree in electrical engineering from the Mohammadia School of Engineers (EMI), Rabat, Morocco, the Aggregation degree in electrical engineering from the ENSET School, in 2003, and the D.E.S.A. degree in industrial electronics from EMI. He is currently a Professor with the Higher National School of Arts and Trades (ENSAM), University of Moulay Ismail, Meknes, Morocco. His research interests include static converters, electrical machines, control systems, and power electronics.

BADRE BOSSOUFI was born in Fez, Morocco, in 1985. He received the Ph.D. degree in electrical engineering from the Faculty of Sciences, Sidi Mohammed Ben Abdellah University, Fez, and the joint Ph.D. degree from the Faculty of Electronics and Computer, The University of Pitesti, Romania, and Montefiore Institute of Electrical Engineering, Liège, Belgium, in 2012. He was a Professor in electrical engineering with the Faculty of Sciences, Sidi Mohamed Ben Abdellah University. His research interests include static converters, electrical motor drives, power electronics, smart grid, renewable energy, and artificial intelligence.

ILHAMI COLAK was born in Turkey, in 1962. He received the Diploma degree in electrical engineering and the M.Sc. degree in electrical engineering in the field of speed control of wound rotor induction machines using semiconductor devices from Gazi University, Turkey, in 1985 and 1991, respectively, the M.Phil. degree from the University of Birmingham, England, in 1991, and the Ph.D. degree in mixed frequency testing of induction machines using inverters from Aston University, England, in 1994. His M.Phil. thesis on high frequency resonant DC link inverters. He became an Assistant Professor, an Associate Professor, and a Full Professor, in 1995, 1999, and 2005, respectively. He has published more than 108 journal articles, 239 conference papers, and seven books in different subjects, including electrical machines, drive systems, machine learning, reactive power compensation, inverter, converter, artificial neural networks, distance learning automation, and alternating energy sources.

THAMER A. H. ALGHAMDI received the B.Sc. degree from Albaha University, Al Baha, Saudi Arabia, in 2012, the M.Sc. degree from Northumbria Newcastle University, Newcastle, U.K., in 2016, and the Ph.D. degree from Cardiff University, Cardiff, U.K., in 2023. Then, he was a Power Distribution Engineer with Saudi Electricity Company (SEC), until 2013. He is currently an Assistant Professor in electrical power engineering with Albaha University, where he was a Lecturer Assistant, from 2016 to 2018. His main research interests include power systems, power quality, the integration of renewables, and AI applications in electrical engineering.

● ● ●